An Introduction to Modern Industrial Mathematics

C. Sean Bohun

Introduction

When beginning this article one of the most difficult questions I was faced with was to provide a definition of industrial mathematics and to distinguish it from applied mathematics. Applied mathematics is primarily concerned with using mathematics as a tool for analysis. This is quite a broad characterization and encompasses not only what one would typically consider the meat and potatoes of modelling physical phenomena, solving problems and interpreting the results, but also finding connections across disciplines and utilizing the language of mathematics to unify disparate fields of study. Theories and models developed in applied mathematics lie at the interface of a deep understanding of mathematical insight and technique with a specialized knowledge of the particular process being studied. Historically, practical applications have led applied mathematicians to develop models which were then taken on by pure mathematicians, where the mathematics was further developed for its own sake. The field has been responsible in the last few decades for opening up completely new disciplines, including everything from string theory to mathematical biology.

There is a further distinction within the discipline of applied mathematics between those that concern themselves with the mathematical methods and the application of mathematics within other fields. This has led to terms such as "practical mathematics" or "applied science" to describe the latter [7], [11]. In this same vein, a possible definition of industrial mathematics is to view it as a subset of applied mathematics where the focus is on the use and development of mathematics to solve industrial problems. I contend that it is more than this.

Industrial mathematics is concerned with *real-world problems* which focus on furthering the establishment and dissemination of links between mathematics and the physical world. The term *industry* is meant in a very broad sense consisting of *any field with either a commercial or societal benefit*, whether it be the optimal design of an electric motor, modelling financial options, or even classifying sociological interactions. The key point to make here is that, despite the inherent complexity of being concerned with real-life problems, industrial mathematics is tasked with laying bare the essential mechanisms at work and effectively disseminating the logical consequences to those *outside* the field of mathematics, significantly increasing understanding in the process.

This definition reflects the evolution of the contact between the industrial community and the mathematical community. What started as an indirect connection through industry hiring professors as consultants and supporting post-doctoral research positions has grown to a global network of modeling workshops where *direct* contact is made between mathematicians and members from industry [5]. Due in part to this effort, there has been a shift in the thinking of the applied mathematics community and in government over the last couple of decades. As evidenced by the 2012 *SIAM Report of Mathematics in Industry* [19], the role of mathematics in industrial society is not only relevant but required.

C. Sean Bohun is associate professor of mathematics at the University of Ontario Institute of Technology. His email address is sean.bohun@uoit.ca.

DOI: http://dx.doi.org/10.1090/noti1096

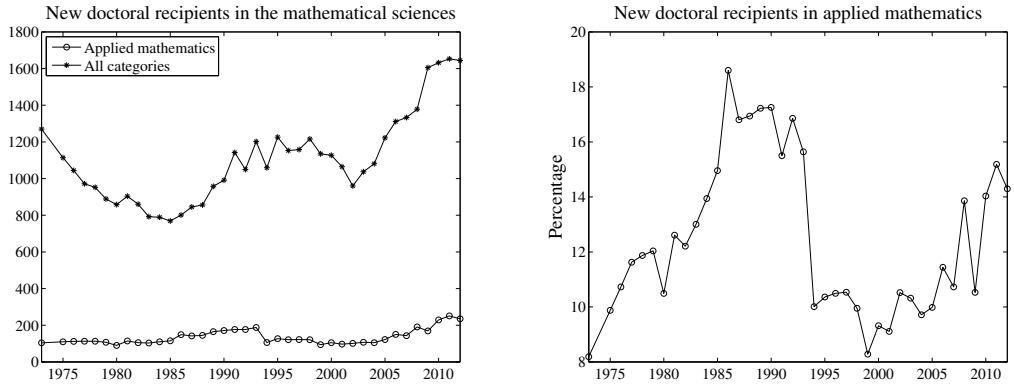

Figure 1. Trends in the number of new doctoral recipients in applied mathematics from 1973 to 2012.

- In 1996 manufacturing accounted for 15.4% of US GDP, while the combination of finance, insurance, and scientific and technical services jointly contributed 12.5%.
- By 2010 the order had reversed, with manufacturing accounting for 11.7% and finance, insurance, and scientific and technical services accounting for 15.9%.

This shift identified by SIAM enhances the fact that the skills attained through the study of applied mathematics are integral to the demands being made by this changing demographic. The SIAM *Careers in Applied Mathematics and Computational Sciences* [18] lists a few of these observations that are repeated below.

- Mathematics has burst the old boundaries that limited what an engineer could design, a scientist could know, or an executive could manage.
- Subtle interactions, masses of data, and complex systems are all within the scope of the tools and ideas of applied mathematics.
- The logical clarity and deductive skills you are being taught in your mathematics classes are exactly the tools required to study these complex real-world problems.

Figure 1 shows data for the last forty years for the U.S., extracted from the annual AMS survey [24]. To the left are the number of new doctoral recipients in applied mathematics compared to those across all of the mathematical sciences, while to the right is the corresponding percentage of recipients in applied mathematics. From 1973 to 1985 the historical record shows a steady increase in the percentage of new graduates in applied mathematics as the total number of graduates in the mathematical sciences decreased, while the number of those in applied mathematics held steady. From 1985 to 1994 the total number of graduates increased, and this trend was matched in the applied mathematics group. During this time period there was a steady increase in the percentage of unemployed, reaching 10.7% in 1994 [8] and stabilizing in 1995 with a sharp drop in graduates in applied mathematics. This drop was not reflected in the mathematical sciences community as a whole. Since the year 2000 there has been a steady increase in the number of graduates in the mathematical sciences, recently surpassing anything in the historical record, yet the same trend has not been seen in applied mathematics. What we as applied mathematicians need to ask ourselves is why. As I have described above, the current trend in funding for applied mathematics is tied to industrial relationships [1], [9], [13], yet this is not a watershed for applied mathematics. I believe this is primarily a problem of public relations and a lack of a unified message across the discipline to expose potential students to the wonder, excitement, personal sense of accomplishment, and basically *fun* of being a part of the worldwide effort to apply modern mathematics to real-life problems.

One of the main difficulties of modern applied and industrial mathematics is not relevance or a lack of interesting problems. Personally, I have found that once students begin to have a sense of the applicability and relevancy of this discipline, the problems themselves become the best recruitment tool of all. In fact, the richness of the mathematics found with many of the problems brought to various study groups around the world have formed the backbone of a number of texts of advanced modeling [5], [7], [10], [11].

In the remainder of this report I will consider two case studies in industrial mathematics to give some insight as to the variety of techniques available to the industrial mathematician. One of these problems had its inception as a real-life problem brought to one of the global network of modeling workshops, while the other began with a seemingly innocuous question from an interested student.

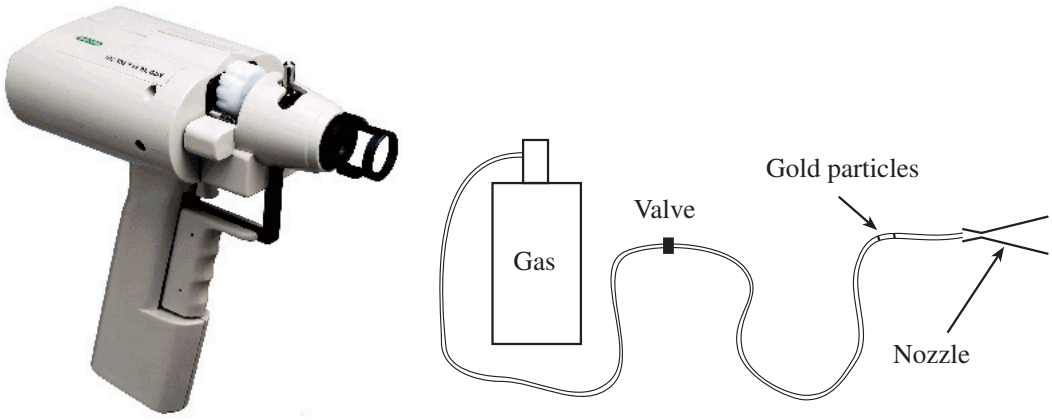

Figure 2. A Helios gas burst gene gun and the underlying gene gun geometry.

The emphasis here is placed on the questions and the process that one goes through when first exposed to any given problem and not on the level of sophistication. In fact, overcomplicating an already complicated problem seems to be a skill that pervades most academic disciplines. If there is a theme in what follows, it is that a deep understanding of simple models as well as their limitations should never be underestimated. What should be clear after reading through the models is that each choice made when modelling has both benefits and disadvantages and the modeller is continually faced with balancing mathematical with practical issues. Effectively navigating through these waters becomes an art as opposed to a science. The first example is taken from the field of biotechnology and is concerned with the design of a gene gun, and my introduction is the following exchange I had with a previous student:

NJ: Dr. Bohun, why do they use helium in a gene gun? Why not just air?

CSB: What's a gene gun?

Let's find out!

Modelling a Gene Gun

A gene gun consists of a tube that is configured to propel DNA-coated microparticles, typically gold, into a wide range of biological samples. There are a number of propulsion methods that have been utilized in the past, including, but not limited to, electric discharge, gunpowder explosions, gas flow and gas burst methods [14], [15], [22]. Figure 2 shows a Helios gas burst gene gun and a diagram of its functionality.

The details of how a gene gun works is a combination of biochemistry and physics. Under certain chemical conditions DNA can become sticky and adhere itself to biologically inert particles, for example, gold. These gold microparticles can act as bullets if they are placed in the path of a pressure pulse. The gas burst gene gun consists of a high-pressure tank of helium, a shock tube, and a nozzle. By placing the microparticles on the interior wall of the shock tube after the valve, the particles accelerate as the shock wave travels down the tube. They then pass through a nozzle made up of a converging and a diverging section, which makes it possible to achieve high-speed gas molecules without having a very high pressure. Different gases can be used to generate a shock wave inside the shock tube, including helium (He), carbon dioxide (CO_2), and air—mainly nitrogen (N_2). But why is helium used? The modeling may provide an answer to this. In this work, we model the behavior of such a device and search for ways in which to optimize the design as a first step in designing a handheld device using a CO_2 cartridge.

A short pressure pulse imparts a drag force on the microparticles that accelerates them through the nozzle and subsequently into the target. Our specific modeling effort will focus on helium as the accelerating gas but also briefly contrast with carbon dioxide. As for the microparticles, we require a high-density material that does not react with our biological sample. Many materials are available as a delivery particle, including tungsten, gold, polystyrene, borosilicate, and stainless steel [14]. Our model will assume the use of gold, since this has the highest density and is available as essentially spherical particles.

Much of the underlying theory of the operation of a gas-burst gene gun is closely related to the concept of a cold spray whereby an ultrafine metal powder is accelerated to supersonic velocities and deposited on the surface of a target material. The interested reader is directed to the text by Papyrin et al. [16] to further explore this connection. Many of the submodels that are cascaded together in this problem contain material that is well trodden, and the reader will be referred to an appropriate classical text when appropriate.

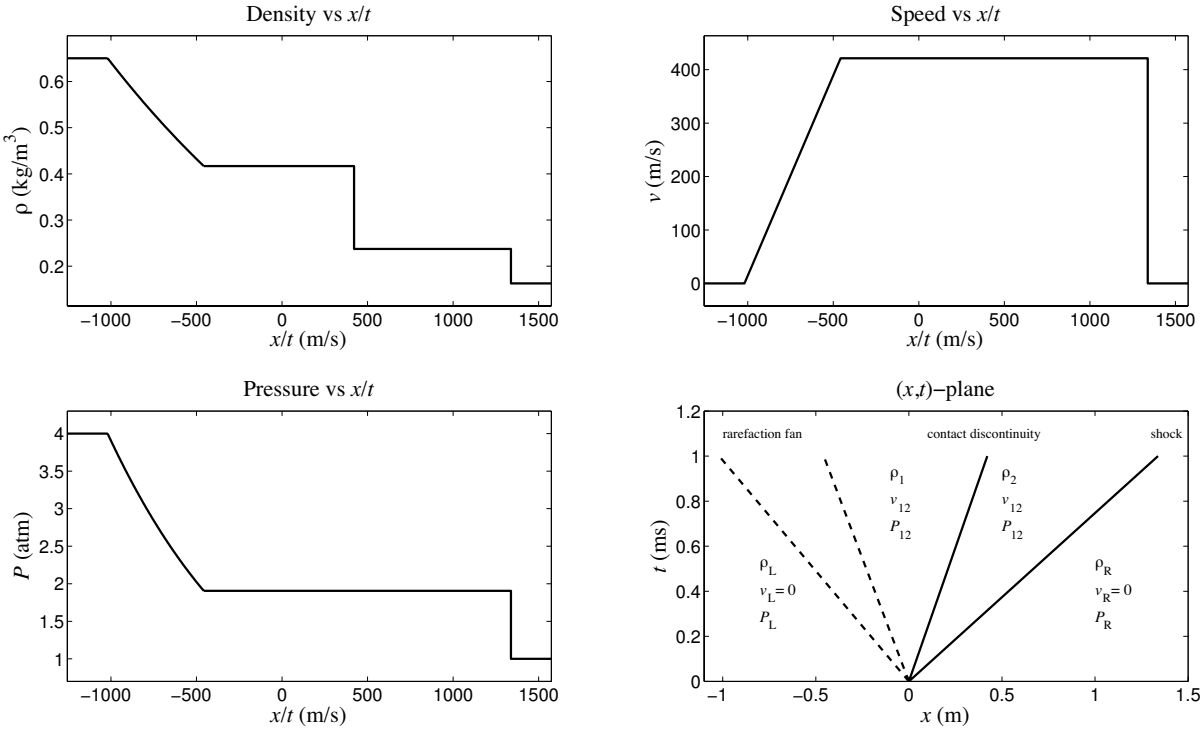

Figure 3. A simulated shock flow of helium gas for an initial uniform temperature of $T_0 = 300$ K. A leading shock in all three variables is followed by a contact discontinuity in the density and finally a trailing rarefaction fan. The bottom right panel shows the structure of the solution in the (x,t)-plane and the piecewise constant values within each of the solution regions.

Shock Tube

The underlying assumptions for the shock tube include:

- the diameter of the tube is much smaller than its length,
- viscosity of the gas is ignored and no heat energy is exchanged within the walls of the tube,
- the tube is considered to be frictionless with respect to the flow of the gas.

The first assumption allows one to reduce the problem to one spatial dimension, whereas the second and third assumptions allow us to assume that the gas flow is *isentropic* (adiabatic and frictionless). Under these assumptions the conservation of mass, momentum, and energy can be expressed as:

$$\text{(1a)} \qquad \frac{\partial \rho}{\partial t} + \frac{\partial}{\partial x}(\rho v) = 0, \qquad \text{(mass)}$$

$$\text{(1b)} \qquad \frac{\partial (\rho v)}{\partial t} + \frac{\partial}{\partial x}\left(\rho v^2 + P\right) = 0, \qquad \text{(momentum)}$$

$$\text{(1c)} \qquad \frac{\partial E}{\partial t} + \frac{\partial}{\partial x}(v(E+P)) = 0, \qquad \text{(energy)}$$

where ρ, v, and P respectively denote the density, speed, and pressure of the gas. The variable E denotes the total energy of the gas per unit volume and can be written as the sum of the gas's internal energy and its kinetic energy. In the case of an isentropic gas,

$$\text{(1d)} \qquad E = \frac{1}{2}\rho v^2 + \frac{1}{\gamma - 1}P,$$

where γ is the ratio of the specific heats. For helium, $\gamma = c_p/c_v = 5/3$.

When the pulse of gas is initiated, we assume that the shock tube is in thermal equilibrium with a room temperature of $T_0 = 300$ K and that the gas is at rest, $v_0 = 0$. Across the valve is a jump of pressure:

$$\text{(2a)} \qquad P(x,0) = \begin{cases} P_L = 4 \text{ atm}, & x < x_0; \\ P_R = 1 \text{ atm}, & x > x_0, \end{cases}$$

where x_0 is the location of the valve in the tube. There is a corresponding initial jump in the gas density, with pressure and density related through the ideal gas equation (1 atm = 101325 Pa):

$$\text{(2b)} \qquad \rho(x,0) = \frac{P(x,0)}{\mathcal{R}T_0} = \begin{cases} \rho_L = 0.6505 \text{ kg m}^{-3}, & x < x_0, \\ \rho_R = 0.1626 \text{ kg m}^{-3}, & x > x_0, \end{cases}$$

with the ideal gas constant for helium, $\mathcal{R} = 8.314 \times 10^3 \text{ JK}^{-1}\text{mol}^{-1}/M_w$, $M_w = 4.003 \text{ g mol}^{-1}$, being the molecular weight of the gas. Finally, at the edges of the spatial domain, we assign a zero Neumann boundary condition that is consistent

provided no disturbance in any of the variables has time to reach the boundary.

A conservation law together with piecewise constant initial data having discontinuities is known as a Riemann problem, and to solve the system (1), it is written in the form

$$\mathbf{u}_t + A\mathbf{u}_x = \mathbf{0} \tag{3a}$$

where $\mathbf{u} = (\rho, \rho v, E)^{\mathrm{T}}$ and [12], [23]

(3b)

$$A = \begin{pmatrix} 0 & 1 & 0 \\ (\gamma-3)\frac{v^2}{2} & (3-\gamma)v & \gamma-1 \\ (\gamma-1)\frac{v^3}{2} - (E+P)\frac{v}{\rho} & (E+P)\frac{1}{\rho} - (\gamma-1)v^2 & \gamma v \end{pmatrix}.$$

The solution is usually presented in terms of the pressure P rather than the less intuitive (for this problem) yet mathematically more convenient total energy E with expression (1d) used to make this exchange.

The described problem is a variant[1] of Sod's [20], and has a well-known exact solution that can be found either in any well-represented gas dynamics text, for example [2], or more recently within the case studies by Danaila et al. [6]. Figure 3 illustrates the structure of the solution, and Table 1 contrasts He and CO_2 where in all cases the initial temperature, pressure differential, and velocity of the gas remain constant: $T_0 = 300$ K, $P_{\mathrm{L}} = 4$ atm, $P_{\mathrm{R}} = 1$ atm, $v_{\mathrm{L}} = v_{\mathrm{R}} = 0$. A shock in all three variables $(\rho, v, P)^{\mathrm{T}}$ propagates at a speed v_{S}, which is then followed by a contact discontinuity in the density moving at $v_{\mathrm{CD}} = v_{12}$ and finally a trailing rarefaction fan in all three variables, the edges of which move at speeds $v_{\mathrm{L}}^{\mathrm{fan}} < v_{\mathrm{R}}^{\mathrm{fan}}$.

The purpose of modeling the shock wave is to provide initial conditions for the gas entering the nozzle. The values obtained are idealized, since both the friction and viscosity have been ignored, yet they give some initial insight for why helium is preferred. It is clear from the data in Table 1 that, for a fixed pressure differential, the initial shock speed of helium is significantly larger than that of air or carbon dioxide. However, it is not only the speed of the gas particles that determines the behavior of the gold microparticles but the density of the gas as well. Since the density of carbon dioxide is nearly ten times that of helium, any clear advantage of using helium remains elusive.

Nozzle Modelling

At the end of its travel down the shock tube the gas is passed through a nozzle, and this changes its speed, pressure, temperature, and density. The model for the shock tube, together with the nozzle, describes the behavior of the gas along the complete length of the gene gun, and within this managed stream of gas, the gold microparticles acquire the inertia to be propelled into a biological sample. We begin by illustrating how a nozzle is used to accelerate the gas particles.

An ideal isentropic gas satisfies the additional relationship $P\rho^{-\gamma} = \text{const.}$ and, as a result, the speed of sound is given by

$$c^2 = \frac{\mathrm{d}P}{\mathrm{d}\rho} = \gamma\frac{P}{\rho} = \gamma\mathcal{R}T \tag{4}$$

using the ideal gas equation of state (2b). For a steady one-dimensional flow through the nozzle, the continuity equation reduces to the hydraulic approximation $\rho v A = \text{const.}$, where A is the cross-sectional area at any point in the nozzle. Expressed in terms of differentials this gives

$$\frac{\mathrm{d}\rho}{\rho} + \frac{\mathrm{d}v}{v} + \frac{\mathrm{d}A}{A} = 0. \tag{5}$$

In the same steady one-dimensional limit, using (4), the conservation of momentum reduces to [21]

$$v\,\mathrm{d}v + \frac{1}{\rho}\,\mathrm{d}P = v\,\mathrm{d}v + \frac{c^2}{\rho}\,\mathrm{d}\rho = 0. \tag{6}$$

Eliminating $\mathrm{d}\rho/\rho$ from (5) and (6) and rearranging give the expression

$$\frac{\mathrm{d}A}{\mathrm{d}v} = \frac{A}{v}\left(M^2 - 1\right), \tag{7}$$

where the *Mach Number* $M = v/c$.

Expression (7) embodies the purpose of the nozzle. Incident gas particles approaching the nozzle at subsonic speeds ($v < c$) are accelerated with the converging portion. If the particles reach the sonic speed ($v = c$) at the throat of the nozzle, then they can be further accelerated to supersonic speeds ($v > c$) with the diverging portion. To summarize, the maximum possible exit velocity of the gas particles is attained by having subsonic flow in the converging part of the nozzle and supersonic flow in the diverging part, and this can only be attained by having $v = c$ at the throat.

Continuing the analysis yields a relationship between the Mach number and the cross-sectional area at any point in the nozzle [2], [21]:

$$\frac{A}{A_*} = \frac{M_*}{M}\left(\frac{1 + \frac{\gamma-1}{2}M^2}{1 + \frac{\gamma-1}{2}M_*^2}\right)^{\frac{\gamma+1}{2(\gamma-1)}} \tag{8}$$

with A_* and M_* denoting the area and Mach number at the throat of the nozzle. If $M_* < 1$, then the gas speeds up as the nozzle narrows and then simply slows down in the diverging part, since A/A_* can never be less than 1 for a converging/diverging nozzle. For $M_* > 1$, the gas must be entering the nozzle faster than the speed of sound and the converging nozzle actually *slows* the gas, contrary to one's intuition. Only in the case $M_* = 1$, when the speed at the throat of the nozzle matches the speed of sound, can

[1] *Sod's original problem has the initial conditions* $\rho_L = 1$, $P_L = 1$, $v_L = 0$, $\rho_R = 0.125$, $P_R = 0.1$, *and* $v_R = 0$.

Gas	γ	M_w (g mol^{-1})	P_{12} (atm)	ρ_1 (kg m^{-3})	ρ_2 (kg m^{-3})
He	1.667	4.003	1.905	0.4169	0.2374
CO_2	1.289	44.01	1.941	4.081	2.969
Gas	v_{12} (m s^{-1})	v_L^{fan} (m s^{-1})	v_R^{fan} (m s^{-1})	v_{CD} (m s^{-1})	v_S (m s^{-1})
He	421.4	−1019	−457.2	421.4	1338
CO_2	145.6	−270.3	−103.6	145.6	366.2

Table 1. Solution to the Riemann problem for He and CO_2. In all cases $T_0 = 300$ K, $P_L = 4$ atm, $P_R = 1$ atm, $v_L = v_R = 0$ and ρ_L, ρ_R follow from the ideal gas law (2b). The speeds of the initial shock, the contact discontinuity, and the left and right edges of the rarefaction fan are denoted by v_S, v_{CD}, v_L^{fan} and v_R^{fan} respectively.

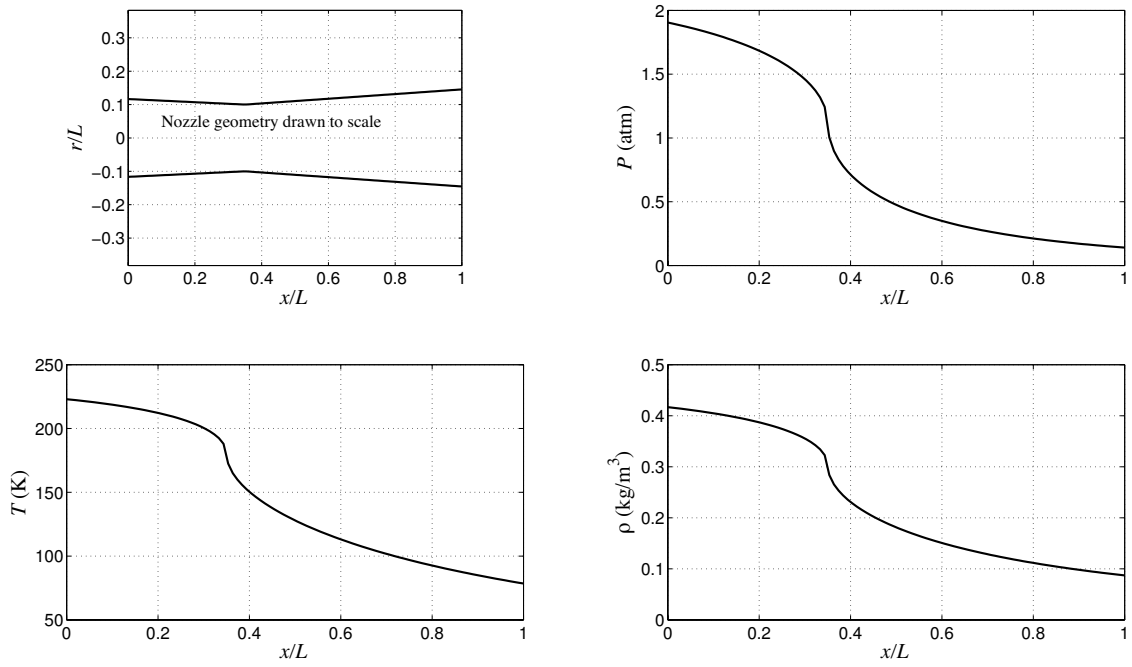

Figure 4. Pressure, temperature, and density for the indicated nozzle design with $L = 2$ cm and assuming the flow of helium gas from the shock tube.

the particles transfer from subsonic ($M < 1$) to supersonic ($M > 1$) speeds. Subsonic particles enter the nozzle, they speed up to Mach-1 at the throat, and they continue to accelerate as the nozzle diverges.

This increase in speed of the gas is done at the expense of a loss of internal energy. What this means is that the temperature, the pressure, and the density of the gas all drop as it progresses through the nozzle. Assuming that $M_* = 1$, these are given by the expressions [21]

$$\begin{aligned} \frac{T}{T_0} &= \frac{1 + \frac{\gamma-1}{2} M_0^2}{1 + \frac{\gamma-1}{2} M^2}, \\ \frac{P}{P_0} &= \left(\frac{T}{T_0}\right)^{\frac{\gamma}{\gamma-1}}, \\ \frac{\rho}{\rho_0} &= \left(\frac{T}{T_0}\right)^{\frac{1}{\gamma-1}}, \end{aligned} \tag{9}$$

where (M_0, T_0, P_0, ρ_0) are the values at the entrance of the nozzle. Connecting the behavior within the nozzle to the results of the shock tube analysis is now simply a matter of matching the nozzle input parameters. That is, $P_0 = P_{12}$, $\rho_0 = \rho_1$, $T_0 = P_{12}/\rho_1 \mathcal{R}$ and setting $M_0 = v_{12}/(\gamma \mathcal{R} T_0)^{1/2}$, where the values are taken from Table 1 for the flow *after* the contact discontinuity has passed. For the simulations a simple converging/diverging nozzle is chosen with an entrance angle consistent with the Mach number of the entering gas and an exit angle of four degrees. The resulting flow for a nozzle of length $L = 2$ cm assuming helium is shown in Figure 4.

One of the important design aspects with nozzle design is to ensure that the pressure does not drop too low, or the outside gas will rush into the nozzle, undoing any advantage of making the gas supersonic in the first place. We will not address

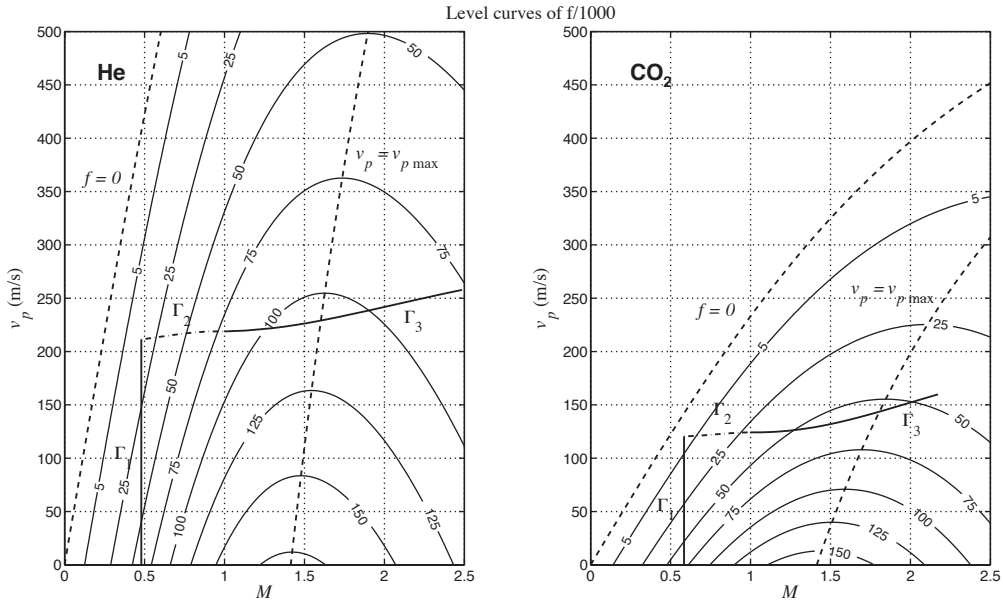

Figure 5. Behavior microparticles when utilizing the simple converging/diverging nozzle depicted in Figure 4. Note that $v_p/c(M) \le M$ for the assumed model of the drag. For this simulation the microparticles are placed 10 cm from the nozzle entrance and the nozzle is 2 cm in length.

this issue of what is referred to as a *normal shock* but refer the reader elsewhere [21].

Drag Force

Having shown how the speed of the gas varies throughout the gene gun apparatus, we can move on to investigating how the gold microparticles are accelerated. By treating the gold particles as tiny spheres that are dragged along by collisions with the gas molecules moving past them and assuming that the microparticles are always moving slower than the gas, we find that the equations of the motion of the gold particles are

(10)
$$\frac{dx_p}{dt} = v_p, \qquad x_p(0) = 0,$$
$$m_p \frac{dv_p}{dt} = \frac{1}{2} C_D A_p \rho (v - v_p)^2, \qquad v_p(0) = 0.$$

This model ignores gravity, since the gold particles are quite small and it is easy to verify that the gravitational force is far outweighed by the force due to the pressure pulse. Quantities m_p, v_p, and A_p are the mass, speed, and cross-sectional area of the gold particles, C_D is the drag coefficient ($C_D \simeq 1$ if the Reynolds number ≥ 30) [21], and (v, ρ) are the speed and density of the gas respectively. These are initially obtained from the shock tube model and subsequently changing within the nozzle, as described above. Typical values for the gold microparticles are [14]

(11a) $\quad r_p = 3 \times 10^{-6}$ m, $\quad \rho_p = 16800$ kg m^{-3}

and the combination

(11b) $\quad C_D \dfrac{A_p}{2m_p} = \Gamma_0 = \dfrac{3}{2 r_p \rho_p} \simeq 29.76$ m^2 kg^{-1}

so that (10) can be written as

(12a)
$$\frac{dx_p}{dt} = v_p, \qquad x_p(0) = 0,$$
$$\frac{dv_p}{dt} = \Gamma_0 f(v_p; M, \rho, c), \qquad v_p(0) = 0,$$

for $v_p < Mc$ where

(12b) $\qquad f(v_p; M, \rho, c) = c^2 \left(M - \dfrac{v_p}{c} \right)^2.$

Figure 5 displays the level curves of $f \times 10^{-3}$ for both He and CO_2. Bounded above by $2c^2$, the admissible domain contains an interior curve along which f attains its maximum value for a fixed value of v_p. A straightforward calculation gives

(13a) $\dfrac{\partial f}{\partial M} = -\gamma P_0 \left(M - \dfrac{v_p}{c} \right) \left(M^2 - \dfrac{v_p}{c} M - 2 \right) \left(1 + \dfrac{\gamma - 1}{2} M^2 \right)^{\frac{1-2\gamma}{\gamma - 1}}$

with

(13b)
$$c = (\gamma \mathcal{R} T)^{1/2} = (\gamma \mathcal{R} T_0)^{1/2} \left(1 + \frac{\gamma - 1}{2} M^2 \right)^{-1/2},$$

giving this curve as

(13c) $\qquad v_{p\,max}(M) = \left(M^2 - 2 \right) \dfrac{c}{M}.$

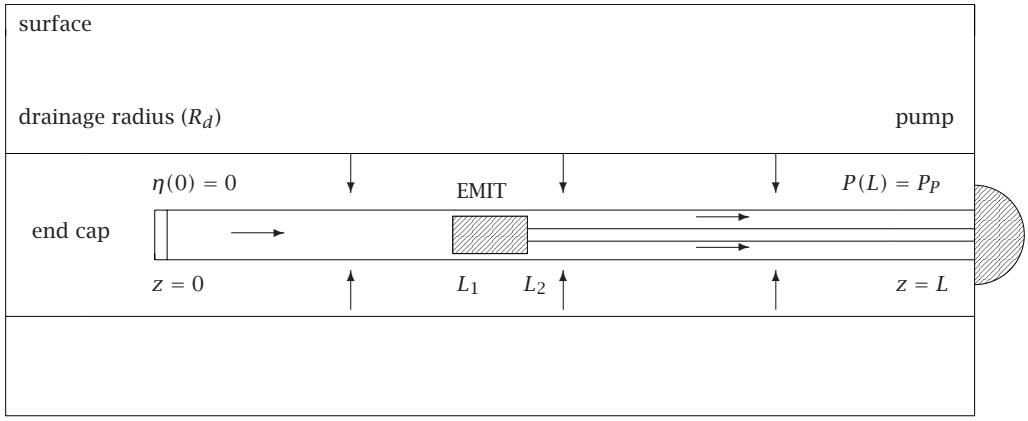

Figure 6. Overall geometry for the horizontal wellbore problem. A horizontal cylindrical well extends from $z = 0$ to $z = L$ with a pump located at $z = L$ to pull the heated oil out of the rock formation.

In each case the trajectory of the microparticles is computed assuming that they initially lie 10 cm from the nozzle entrance and the nozzle is 2 cm in length. Three distinct regions characterize the behavior.

1. Approaching the nozzle, the gas flow is constant and the gold particles accelerate towards the nozzle entrance. In this regime the speed of the microparticles is given by (12) with a fixed Mach number determined by the solution of the shock tube equations. The final speed in this region is determined by the initial distance of the microparticles to the nozzle entrance. Within He the microparticles only achieve 50% (211 $\mathrm{m\,s^{-1}}$) of the gas flow speed of (421 $\mathrm{m\,s^{-1}}$), whereas the higher density of CO_2 allows the microparticles to reach 82% (120 $\mathrm{m\,s^{-1}}$) of the gas flow speed (146 $\mathrm{m\,s^{-1}}$) over the same distance.
2. In the converging section of the nozzle the gas particles rapidly approach $M = 1$, and in both cases of He and CO_2 this occurs over such a short timeframe (He : 32 μs, CO_2 : 57 μs) that no significant change in microparticle speed occurs.
3. In the diverging section the shape of the nozzle can be modified to allow the microparticles to track the curve of maximal drag curve. Again this portion of the nozzle is quickly traversed (He : 55 μs, CO_2 : 92 μs) so that only a moderate increase is observed.

With the groundwork that has been laid, a nozzle design that maximizes the exit velocity of the microparticles can be determined. This design will clearly depend on the gas being used. There are other issues as well. First, the gold particles are not uniform in size, and their diameters will have some probability distribution. We may wish to investigate the effect of this fact in the current model. Second, we have only begun the investigation of contrasting the effect of the use of other gases. And finally, we have not even started to consider a model for stopping the particles and controlling the distribution of where they embed themselves in a target.

Clearly, for validation of the model a set of data needs to be made available and the predictions of the model compared to what is seen experimentally. Let's return to the student's initial question: "Why do they use helium in a gene gun?" The simple answer is the structure of the gas and its nonreactivity. Helium, being a noble gas, will not easily react with a biological sample, but this is not the only reason. The structure of the gas (essentially spheres) gives a value of $\gamma = 5/3 \simeq 1.67$. Carbon dioxide molecules are slightly more complicated, with two oxygen atoms connected to a single carbon atom. The result is a value of $\gamma = 7/5 = 1.4$. The larger value of γ makes helium more efficient in that less energy goes into the internal vibrations of the molecules and consequently there is a larger Mach number for a given area ratio. So now you know!

Horizontal Wellbore

This last case study was brought to the attention of the author at a problem-solving workshop concerned with primarily oil and gas problems. As oil wells age it becomes increasingly difficult to extract oil from them, and they are eventually abandoned when the cost of extraction becomes prohibitive. To increase the production rate for these wells and ultimately increase their lifespan, one possible technique is to somehow heat the trapped oil, allowing it to flow more easily. The heating technique described to the working group was the use of electromagnetic heaters known as EMIT (electromagnetic induction tool) units. For a horizontal well of up to a kilometre in length the practice is to insert several EMIT units at intervals

of about one hundred meters and then power them all from a single cable protected by a steel housing. Figure 6 shows a cut-away section of a well with a single EMIT region. Arrows indicate the flow of oil that seeps into the well from the surrounding rock subsequently removed from the rock formation with a pump located at $z = L$.

So why do any modelling at all? In this case, the industrialist has an expensive computational fluid dynamics (CFD) code that can be used to simulate the process, but he wants a simplified model that still captures most of the physics. His key requirement is a formulation of the problem that can be solved rapidly so that one can quickly search wide ranges of possible operating parameters. Attempting this with a large commercial CFD software package would become prohibitively expensive. Another application of the model would be financial. Being able to quickly estimate the increase in production by heating the well, one can use the local cost of electrical power to determine the expected profit in a systematic way. As in the previous model, the problem naturally breaks into several subtasks, but in this case they remain intimately coupled throughout the wellbore.

Axial Flow

We start with estimating the amount of oil that will flow into the well over a very short length of time. This is given by an expression originally developed by Peaceman [4], [17] that depends on the drainage radius of the formation; R_d, the outer radius of the well, R_c; the axial length of the section under consideration; and the pressure in the pipe $P(z)$. The expression for a segment of the well with axial length Δz is

$$\Delta\eta(z) = \frac{2\pi k\,(P_R - P(z))}{\mu_0 \ln(R_d/R_c)}\Delta z, \tag{14}$$

where $\Delta\eta$ is measured in $\mathrm{m}^3\,\mathrm{s}^{-1}$, and k, μ_0 are the permeability of the ground and viscosity of the oil respectively. The subscript zero for the viscosity refers to unheated oil, as we have assumed that the fluid seeping into the well is not effectively heated when compared to the fluid flowing along the well. P_R is known as the reservoir pressure and is the minimum suction pressure required to pull oil out of the well. It can vary from one well to the next and increases as the well ages.

Figure 7 illustrates a small section of the well in either the EMIT region or a region with the cable housing. Of course the regions with neither an EMIT nor the housing will not have any blockage. The volumetric flux is given by $\eta(z) = \pi(R_w^2 - R_z^2)\bar{v}$, where $\bar{v}$ is the radially averaged axial velocity, R_w is the inner pipe radius, and R_z depends on whether there is nothing ($R_z = 0$), an EMIT ($R_z = R_e$), or the cable housing ($R_z = R_h$) within the pipe. By the conservation of mass, the amount of fluid that emerges from this infinitesimal segment must be the sum of the fluid that entered along the well and the fluid that seeped in through the sides. In other words,

$$\eta(z_* + \Delta z) = \eta(z_*) + \frac{2\pi k\,(P_R - P(z))}{\mu_0 \ln(R_d/R_c)}\Delta z \tag{15}$$

or, letting $\Delta z \to 0$,

$$\frac{\mathrm{d}\eta}{\mathrm{d}z} = \frac{2\pi k\,(P_R - P(z))}{\mu_0 \ln(R_d/R_c)}, \qquad \eta(0) = 0. \tag{16}$$

The condition $\eta(0) = 0$ simply reflects the fact that at the end cap the only flux of oil is that dripping in from the sides.

Axial Pressure

Assuming a steady state solution, the Navier-Stokes equations provide a connection between the fluid flow and the pressure drop applied to the fluid. The axial velocity of the fluid depends on its radial position in the well and for the EMIT and housing regions. By further assuming that the radial flow entering the well from the sides is much smaller than the axial flow (strictly true only away from the sidewall), it then satisfies

$$\mu\frac{1}{r}\frac{\partial}{\partial r}\left(r\frac{\partial v}{\partial r}\right) = \frac{\mathrm{d}P}{\mathrm{d}z}, \quad v(R_w) = 0, \quad v(R_z) = 0, \tag{17}$$

where R_z is either the EMIT or the housing radius with the solution

$$v(r) = \frac{1}{4\mu}\frac{\mathrm{d}P}{\mathrm{d}z}\left[r^2 - R_w^2 + \frac{R_w^2 - R_z^2}{\ln(R_w/R_z)}\ln\left(\frac{r}{R_w}\right)\right]. \tag{18a}$$

For regions where $R_z = 0$ we impose the condition $v(0) < \infty$ to find that

$$v(r) = \frac{1}{4\mu}\frac{\mathrm{d}P}{\mathrm{d}z}(r^2 - R_w^2). \tag{18b}$$

Computing the average radial velocity defined as

$$\bar{v} = \frac{2}{R_w^2 - R_z^2}\int_{R_z}^{R_w} v(r) r\,\mathrm{d}r, \tag{19}$$

using $\eta = \pi(R_w^2 - R_z^2)\bar{v}$, and solving for the pressure give

$$\frac{\mathrm{d}P}{\mathrm{d}z} = -\frac{8\mu}{\pi R_w^4}\left[\frac{\ln\lambda}{(1-\lambda^2)^2 + (1-\lambda^4)\ln\lambda}\right]\eta(z), \qquad P(L) = P_P, \tag{20}$$

where $\lambda = R_z/R_w$ is piecewise constant and P_P is the suction applied by the pump at the surface $z = L$. Combining this with expression (16) we obtain a two-point boundary value problem

$$\frac{\mathrm{d}^2\eta}{\mathrm{d}z^2} - \gamma^2(z)\frac{\mu}{\mu_0}\eta = 0, \qquad \eta(0) = 0, \qquad \left.\frac{\mathrm{d}\eta}{\mathrm{d}z}\right|_L = \frac{2\pi k(P_R - P_P)}{\mu_0 \ln(R_d/R_c)}, \tag{21a}$$

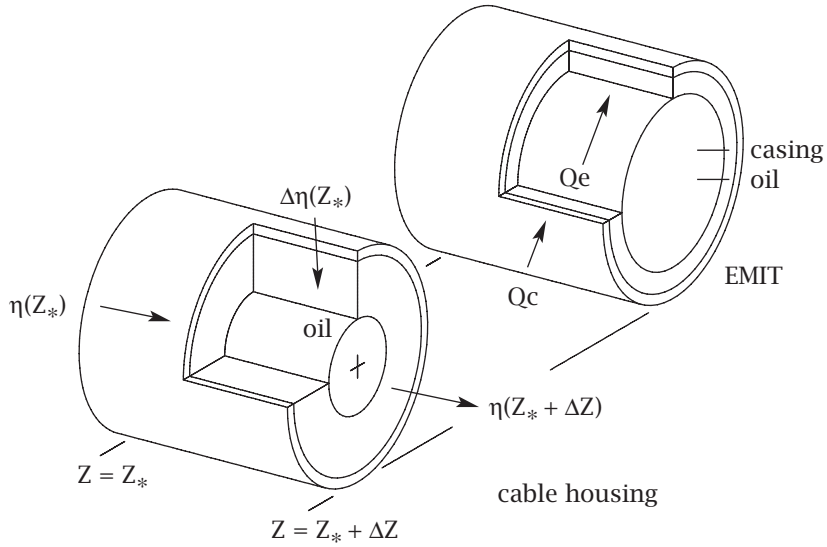

Figure 7. Axial flow within the well illustrating both the fluid flow and the power flux from the casing and the EMIT.

where

(21b)

$$\gamma^2 = \frac{16k}{R_w^4 \ln(R_w/R_c)} \frac{\ln\lambda}{(1-\lambda^2)^2 + (1-\lambda^4)\ln\lambda}$$

is piecewise constant, reflecting the placement of EMIT, housing, and free regions.

Heating the Wellbore

How do we deal with the heat that is being generated in the wellbore? Since we know where the oil is flowing, we can determine the heat flux

(22a) $$\Phi = -k_o \nabla T + \rho C_p \mathbf{v} T,$$

where T is the temperature, $\mathbf{v}$ is the fluid, and k_o, ρ, C_p are respectively the thermal conductivity, density, and heat capacity of the oil. The heat equation can be written in terms of this flux as

(22b) $$\frac{\partial}{\partial t}(\rho C_p T) + \nabla \cdot \Phi = Q,$$

where Q corresponds to an external heating source. To find an effective axial temperature the flux in each of the four regions (reservoir, casing, well, EMIT) is determined and combined with a radial averaging process. The resulting final expression for the average temperature is obtained in [3], where it is shown to satisfy

(23)

$$\rho C_p \frac{\mathrm{d}}{\mathrm{d}z}(\eta(z)T(z)) = \pi\left(Q_c(z)\left(R_c^2 - R_w^2\right) + Q_e(z)R_e^2\right),$$
$$T(0) = 0.$$

The heat sources Q_c and Q_e have been written as functions of z; if one is not in an EMIT region, these functions are simply zero. As a result, the right-hand side of (23) is piecewise constant and nonzero only where an EMIT is located. In addition, the temperature scale is chosen so that $T = 0$ corresponds to 25°C. Integrating (23) for a single EMIT region extending from L_1 to L_2 gives the result that

(24)

$$T(z) = \begin{cases} 0, & 0 \le z < L_1, \\ \frac{\pi\Omega}{\eta(z)}(z - L_1), & L_1 \le z < L_2, \\ \frac{\pi\Omega}{\eta(z)}(L_2 - L_1), & L_2 \le z \le L, \end{cases}$$

$$\Omega = \frac{Q_c\left(R_c^2 - R_w^2\right) + Q_e R_e^2}{\rho C_f},$$

Data	Symbol	Value
Outer casing radius	R_c	69.85 mm
Inner casing radius	R_w	63.50 mm
EMIT radius	R_e	50.80 mm
Housing radius	R_h	31.1625 mm
Wellbore length	L	1000 m
Permeability	k	9.869×10^{-12} m^2
Ambient viscosity	μ_0	15 Pa s
Drainage radius	R_d	100 m
Reservoir pressure	P_R	5.0×10^6 Pa
Producing pressure	P_P	5.0×10^5Pa
Fluid heat capacity	ρC_p	2.8×10^6 J m^{-3}K^{-1}
Casing power	Q_c	795.8 kW m^{-3}
EMIT power	Q_e	79.58 kW m^{-3}

Table 2. Wellbore, reservoir and thermal properties for a single EMIT region extending from L_1 = 495 m to L_2 = 505 m.

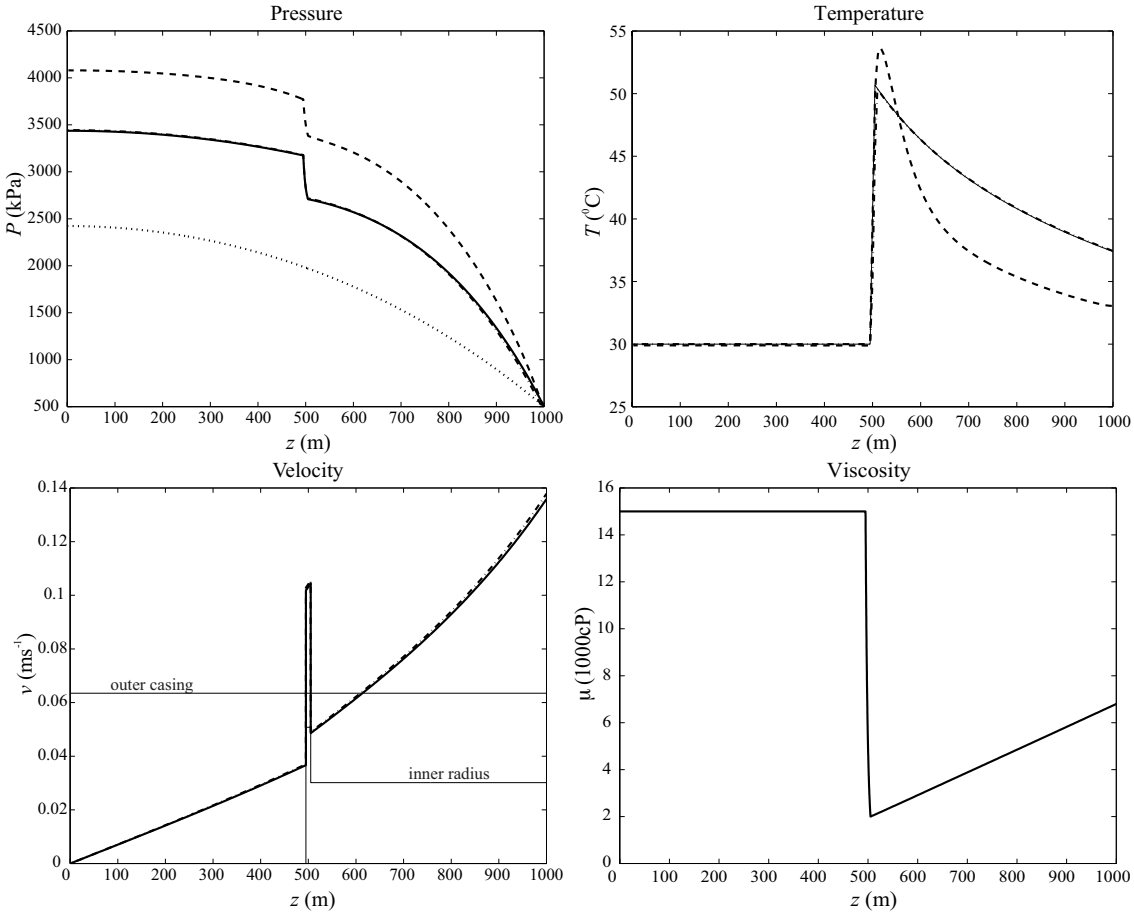

Figure 8. The four figures are the pressure, temperature, velocity, and viscosity as a function of distance along the wellbore. Only the pressure and temperature for the CFD code were available. These are the dashed lines in the respective plots. More than one method was used to solve the simplified model. Where they are distinguishable, the shooting method solution is a solid line, whereas the SOR method is indicated with a dashed dot. A longitudinal section of the wellbore is indicated in the plot of the velocity.

and from this the viscosity μ satisfies the empirical relationship in units of thousands of centipoise[2] through

$$\log_{10}\mu(T) = -3.002 + \left(\frac{453.29}{303.5 + T}\right)^{3.5644}, \tag{25}$$

which closes the model.

Results

To compare the results of the model with the CFD code, a single EMIT unit was placed in the well and the resulting temperature and pressure profiles were calculated. Table 2 lists the various parameters for the model, and Figure 8 shows the resulting pressure, temperature, velocity, and viscosity of the fluid in the well and compares it with the results of the CFD code (dashed lines) in the pressure and temperature plots. The solid and dashed-dot curves (where discernible) correspond to two different techniques for solving the boundary value problem: namely, a shooting method and an SOR method. Both the pressure and the temperature are reasonably well reproduced considering the relative simplicity of the new model. The simplified model underestimates the production rate at the pump giving $\eta_{\mathrm{CFD}}(L) = 187.6\ \mathrm{m^3\,day^{-1}}$ while $\eta(L) = 115.2\ \mathrm{m^3\,day^{-1}}$.

The simplified model reproduces the overall characteristics of the full model described by the CFD code and does this with a comparatively low computational cost. One of the primary benefits of this reduction in the computational cost is that it allows one to run a number of numerical experiments cheaply and onsite in the vicinity of the well itself. The question of determining the optimal placement and number of required EMIT

[2] 1 *centipoise* = 1×10^{-3} *kg m*$^{-1}$ *s*$^{-1}$.

regions for a given production rate is explored in Bohun et al. [3].

Final Words

Despite the ever-increasing complexity and cross-disciplinary nature of modern real-life problems and a redoubling of efforts by government and industry to form meaningful collaborative bridges with mathematicians, the historical record shows that such efforts are being achieved only modestly. Industrial mathematicians weave disparate threads of science from many different fields to produce innovative models which are typically utilized outside the discipline, enriching understanding. Leading the reader through two separate case studies, I have attempted to expose some of the inner workings to encourage students and faculty to participate in the global network of modeling workshops. What has not been emphasized is the importance of building and maintaining working relationships with both industry and other disciplines within academia. With collaboration, both academically and institutionally, we stand to increase not only the range of real-world problems that are made available to us, but we also stand to ensure our positive impact on commercial and societal benefits. Personally I take great satisfaction in seeing the technologies I know and love being applied in productive and interesting ways to real-world problems.

References

1. K. Allen, National Research Council 'open for business,' Conservative government says, May 7, 2013, Accessed: 25/06/2013.
2. J. D. Anderson, *Modern Compressible Flow with Historical Perspective*, McGraw-Hill, 2002.
3. C. S. Bohun, B. McGee, and D. Ross, Electromagnetic wellbore heating, *Canadian Applied Mathematics Quarterly* **10** (2002), 353–374.
4. Z. Chen, *Reservoir simulation: Mathematical techniques in oil recovery, CBMS-NSF Regional Conference Series in Applied Mathematics*, 77, Society for Industrial and Applied Mathematics, 2007.
5. E. Cumberbatch and A. Fitt, *Mathematical Modeling: Case Studies from Industry*, Cambridge University Press, 2001.
6. I. Danaila, J. Pascal, S. M. Kaber, and M. Postel, *An Introduction to Scientific Computing*, Springer Science+ Business Media, 2007.
7. A. C. Fowler, *Mathematical Models in the Applied Sciences*, Vol. 17, Cambridge University Press, 1997.
8. J. D. Fulton, 1995 Annual AMS-IMS-MAA Survey (Second Report), 1995, Accessed: 15/06/2013.
9. The Globe and Mail, How Harper and Obama are alike on science policy, June 7, 2013, Accessed: 25/06/2013.
10. E. Van Groesen and J. Molenaar, *Continuum Modeling in the Physical Sciences*, Vol. 13, Society for Industrial and Applied Mathematics, 2007.
11. S. Howison, *Practical Applied Mathematics: Modelling, Analysis, Approximation*, Vol. 38, Cambridge University Press, 2005.
12. R. J. LeVeque, *Numerical Methods for Conservation Laws*, Birkhäuser, 1992.
13. B. McKenna and I. Semiuk, Research Council's makeover leaves Canadian industry setting the agenda, May 7, 2013, Accessed: 25/06/2013.
14. T. J. Mitchell, M. A. F. Kendall, and B. J. Bellhouse, A ballistic study of micro-particle penetration to the oral mucosa, *International Journal of Impact Engineering* **28** (2003), no. 6, 581–599.
15. S. M. Nabulsi, N. W. Page, A. L. Duval, Y. A. Seabrooks, and K. J. Scotts, A gas-driven gene gun for microprojectile methods of genetic engineering, *Measurement Science and Technology* **5** (1994), no. 3, 267.
16. A. Papyrin, V. Kosarev, S. Klinkov, A. Alkhimov, and V. M. Fomin, *Cold Spray Technology*, Elsevier Science, 2006.
17. D. W. Peaceman, Interpretation of well-block pressures in numerical reservoir simulation (includes associated paper 6988), *Old SPE Journal* **18** (1978), no. 3, 183–194.
18. SIAM, *Careers In Applied Mathematics & Computational Sciences*, Society for Industrial and Applied Mathematics, 1997.
19. _____, The SIAM report on mathematics in industry, 2012, Accessed: 20/12/12.
20. G. A. Sod, A survey of several finite difference methods for systems of nonlinear hyperbolic conservation laws, *Journal of Computational Physics* **27** (1978), no. 1, 1–31.
21. V. L. Streeter, *Handbook of Fluid Dynamics*, McGraw-Hill, 1961.
22. J. L. Thomas, J. Bardou, S. L'hoste, B. Mauchamp, and G. Chavancy, A helium burst biolistic device adapted to penetrate fragile insect tissues, *Journal of Insect Science* **1** (2001).
23. J. W. Thomas, *Numerical Partial Differential Equations: Finite Difference Methods*, Vol. 1, Springer Verlag, 1995.
24. Various, Annual Survey of the Mathematical Sciences, 2012, Accessed: 15/06/2013.